Theoretical calculation of oxygen K electron-energy-loss near-edge structures of Si-doped MgO

1999 J. Phys.: Condens. Matter 11 5661

(http://iopscience.iop.org/0953-8984/11/29/313)

J. Phys.: Condens. Matter **11** (1999) 5661–5670. Printed in the UK PII: S0953-8984(99)00033-8

Theoretical calculation of oxygen K electron-energy-loss near-edge structures of Si-doped MgO

Teruyasu Mizoguchi†, Isao Tanaka‡, Masato Yoshiya†, Fumiyasu Oba† and Hirohiko Adachi†

† Department of Materials Science and Engineering, Kyoto University, Sakyo, Kyoto 606-8501, Japan

‡ Department of Energy Science and Technology, Kyoto University, Sakyo, Kyoto 606-8501, Japan

Received 9 December 1998

Abstract. Maximum solubility of Si in MgO has been reported to be 9.0 at.%. The local environment of the Si solute is of great interest. In order to foresee the difference of the O K-edge electron-energy-loss near-edge structure (ELNES) or x-ray absorption near-edge structure (XANES) due to the presence of the Si solute, first-principles molecular orbital calculations are performed using model clusters composed of 27 and 125 atoms that include a core hole. Extra peaks are found in the theoretical O K-edge photoabsorption cross section (PACS) of the Si-doped cluster. Their positions are found to depend strongly on the Si–O bond length. A realistic model cluster for the Si-doped MgO is constructed by total energy minimization using interatomic potentials. An Mg vacancy is included to keep the charge neutrality. The extra feature in the O K-edge PACS due to the presence of Si is then expected to be located mainly at the higher-energy shoulder of the main peak of the undoped MgO.

1. Introduction

Solid solubility of Si^{4+} in MgO has been reported to be 9.0 at.% at the eutectic temperature of MgO (periclase) and Mg_2SiO_4 (forsterite), that is 2133 K [1]. Si^{4+} in SiO_2 usually exhibits fourfold coordination except for the high-pressure form, known as stishovite. On the other hand, Mg^{2+} in MgO shows sixfold coordination. When Si^{4+} is dissolved into MgO by substituting the Mg^{2+} site, Si^{4+} can be expected to occupy the sixfold coordination site. A trial to detect the sixfold coordinated Si was reported by Kaneko *et al* [2] at the grain boundary of Si-doped Al_2O_3 ceramics. Si was found to segregate at the grain boundary showing signs of sixfold coordination by the spatially resolved electron-energy loss near-edge structure (ELNES) at the O K edge. Because of the localization of the Si in the Si-doped Al_2O_3 ceramics and very high susceptibility to irradiation damage, detailed study of the doped Al_2O_3 was not possible to complete. MgO as a host may be much easier to investigate since Si was reported to show rather high solubility. In the present study, prior to the experimental work, we calculate the theoretical ELNES for the Si^{4+}-doped MgO system.

An electron energy loss spectrometer (EELS) is often installed in a modern transmission electron microscope (TEM). Under ordinary experimental conditions of TEM, the near-edge structure of EELS is similar to XANES (x-ray absorption near-edge structure). In the core-loss process, an electron is excited from a core level to an unoccupied state by electric dipole

0953-8984/99/295661+10$30.00

transition. As a result, experimental ELNES is related to the unoccupied partial density of states of the selected atom that is allowed by the electric dipole selection rule.

First-principles cluster calculations on the basis of molecular orbital (MO) theory have been successful for reproduction of O K-edge ELNES of some oxides [3–7]. Core-hole effects can be rigorously included in the self-consistent calculations, which were pointed out to be essential for the ELNES calculation [5–7]. Since the excited electron is localized near the core hole, cluster calculations should be advantageous for ELNES reproduction as compared with some more sophisticated band-structure methods on the basis of the structural unit cell when a core hole is not included.

In the present study, major efforts are focused on O K-edge ELNES. Mg L_{23}, K and O K-edge ELNES or XANES can be commonly investigated for both undoped and doped MgO systems. Since oxygen is directly bound to Si, the O K-edge spectrum may exhibit greater effects than spectra from the Mg edges. Si L_{23}-edge spectra may also provide information on the chemical environment of Si directly. However, experimental complexity due to the superposition of the Si L_{23}-edge spectra with the high-energy tail of the Mg L-edge spectra should be encountered.

In order to understand the orbital interactions most clearly, present calculations are done using a minimal basis set that is generated by solving the radial part of the Schrödinger equation for atoms at each self-consistent iteration. Thus they are flexible to the given chemical environment. We found that the present calculation reproduces satisfactorily the O K near-edge structure of MgO up to about 20 eV above the edge. Its major features are well explained by orbital interactions inside the small clusters.

2. Computational procedures

First-principles MO calculations were made for MgO and Si^{4+}-doped MgO using model clusters composed of 27 and 125 atoms. The excited atom for the corresponding core loss was put at the centre of the clusters. Model clusters were embedded in point charges located at the external atomic sites so as to produce an effective Madelung potential. A program SCAT [8] based on the discrete variational X_α (DV-X_α) method [9] was employed in which numerical atomic orbitals (NAOs) were used as basis functions. They were generated flexibly by solving the radial part of the Schrödinger equation for a given environment. Minimal basis sets were used in order to clarify the simple relationship between spectral features and chemical bondings. Basis sets were 1s, 2s and 2p for O and 1s, 2s, 2p, 3s, 3p and 3d for Mg and Si. Integrations to obtain energy eigenvalues and eigenfunctions were made in a numerical manner.

In the electron-energy-loss process, an electron is promoted from a core level to an unoccupied state leaving a core hole. As a result, electronic structure in this state differs from that of the ground state. In order to reproduce the experimental spectrum, self-consistent calculation should be carried out including a core hole. The difference in total energies between initial and final states (transition energy) is well approximated as the difference in molecular orbital (MO) energies calculated for the Slater transition state [10] where half of an electron is removed from a core orbital to put into an unoccupied MO. In order to compute the absolute transmission energy, temporary spin polarization associated with the electronic transition was taken into account. In other words, spin-unrestricted calculations were made for the core-hole states.

The overlap population between the ith atomic orbital and jth atomic orbital at the ℓth MO is given by

$$Q_{ij}^{\ell} = C_{i\ell} C_{j\ell} S_{ij} \tag{1}$$

where S_{ij} is the overlap integral given by

$$\int \chi_i^*(\boldsymbol{r})\chi_j(\boldsymbol{r})\,\mathrm{d}\boldsymbol{r} = S_{ij}. \tag{2}$$

χ_i and $C_{i\ell}$ are the ith atomic orbital and its coefficient for the ℓth MO.

The oscillator strength I_{ij} for the electric dipole transition for photon absorption between states i and j is given by

$$I_{ij} = \tfrac{2}{3}\Delta E|\langle j|\boldsymbol{r}|i\rangle|^2 \tag{3}$$

where ΔE represents the transition energy. In the present work, I_{ij} was obtained directly by the numerical integration of the dipole matrix. The photo-absorption cross section (PACS) that we need is proportional to the oscillator strength I_{ij}.

Discrete energy eigenvalues can be computed by the MO calculation. In order to visualize the density of states, discrete energy levels were broadened by the Lorenzian function with FWHM of 1.0 eV. PACS and overlap population diagrams were made in the same way by broadening the quantities at discrete levels given by equations (2) and (1), respectively.

Atomic relaxation around Si^{4+} with an Mg vacancy was evaluated by energy minimization using interatomic potentials. A program GULP developed by Gale [11] was used. Interatomic potentials of Buckingham type for Mg–O, Mg–Mg, O–O and Si–O given by Kawamura [12]† were used. In the GULP program, the crystal that surrounds the defect is divided into three spherical regions, namely regions 1, 2a and 2b. In region 1 all atomic interactions are treated exactly. In region 2a the ions are assumed to be situated in a harmonic well. In region 2b only the implicit polarization of sub-lattices, rather than specific ions, is taken into consideration. The radii of spherical regions 1, 2a were chosen to be 0.8, 2.0 nm, respectively. The energy of region 2b was evaluated using a method analogous to the Ewald sum until infinity.

3. ELNES of MgO

Before comparing experimental ELNES with theoretical results, calculated PDOS and PACS are compared. Local PDOS of the core-hole atom is used. When minimal number of atomic orbitals are used as basis functions, the PACS may be well approximated by the local PDOS that is allowed by the selection rule, $\Delta\ell = \pm 1$. In the present computational method, basis functions are a minimal number of atomic orbitals that are generated flexibly by solving the radial part of the Schrödinger equation for a given chemical environment. Therefore, the PACS can be well approximated by the PDOS in many systems as reported previously [5–7].

The calculated O 2p unoccupied PDOSs and PACS are compared with the experimental O K-edge ELNES [13] in figure 1. Computations were made for two kinds of cluster, i.e. $(OMg_6O_{12}Mg_8)^{2+}$ and $(OMg_6O_{12}Mg_8O_6Mg_{24}O_{24}O_{12}Mg_{24}O_8)^{2-}$ both centred by an oxygen atom. A half-filled O 1s core hole is included. In other words, computations were made for

† Inter-atomic potential U_{ij} is given by

$$U_{ij}(r_{ij}) = \frac{z_i z_j e^2}{r_{ij}} + f_0(b_i + b_j)\exp\left(\frac{a_i + a_j - r_{ij}}{b_i + b_j}\right) - \frac{c_i c_j}{r_{ij}^6}$$

where parameters are given as follows.

	a	b	c	z
O	1.626	0.085	20	−2
Mg	1.161	0.08	2	2
Si	1.012	0.08	0	4

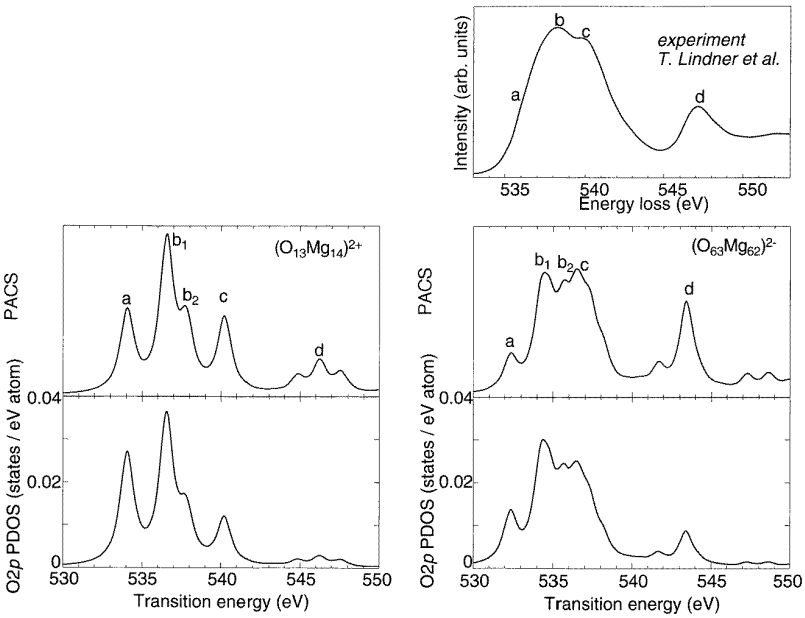

Figure 1. Comparison of the experimental oxygen K-edge ELNES by Lindner *et al* [13] from MgO, theoretical O 2p PDOS and O K-edge PACS calculated for two model clusters. Calculations are made for Slater's transition state.

Slater's transition state. As can be seen, PACS is well approximated by the PDOS except for difference in intensities in the high-energy region. This fact implies that the cross-transitions from O 1s to unoccupied Mg orbitals are almost negligible in the energy region we are interested in. Four peaks denoted by a to d can be found in the experimental spectrum in the energy range of 20 eV from the edge. They are reproduced by the calculation using the smaller cluster. The agreement is improved when a larger cluster is used. The absolute transition energy by the present calculation agrees with the experimental result within an error of 4 eV that is less than 1% of the transition energy.

Spectral features that appear in the O K-edge ELNES can only be understood through the investigation of Mg–O covalent interactions. The Mg 3s, 3p and 3d are the dominant components for orbitals in the energy range of interest. The O 2p is the minor component that is made predominantly by anti-bonding interaction with Mg 3spd orbitals. Figure 2 shows the DOS together with overlap population diagrams for the Mg–Mg and Mg–O bonds calculated for the smaller cluster at the Slater transition state. Peak b can be divided into two sub-peaks, b_1 and b_2, based on their origin. Mg 3s is the dominant component for peaks a and b_1. Mg 3p is dominant for peaks b_2 and c. Mg 3d is dominant for peak d. Separation of peaks a and b_1 can be ascribed to the manner of Mg 3s–Mg 3s interactions. The interaction is bonding for the peak a and antibonding for the peak b_1. Wavefunctions responsible for peaks a and b_1 are shown in figure 3. The molecular orbitals responsible for these peaks by the calculation of the $(O_{13}Mg_{14})^{2+}$ cluster under octahedral (O_h) symmetry are $15t_{1u}$ and $16t_{1u}$ that are triply degenerate orbitals. The wavefunctions shown in figure 3 are one of these triplets. Assignment of all peaks can be made in a similar manner from the viewpoint of interatomic bondings. The present type of molecular orbital calculation is advantageous for providing physical insight for the origin of the spectral features.

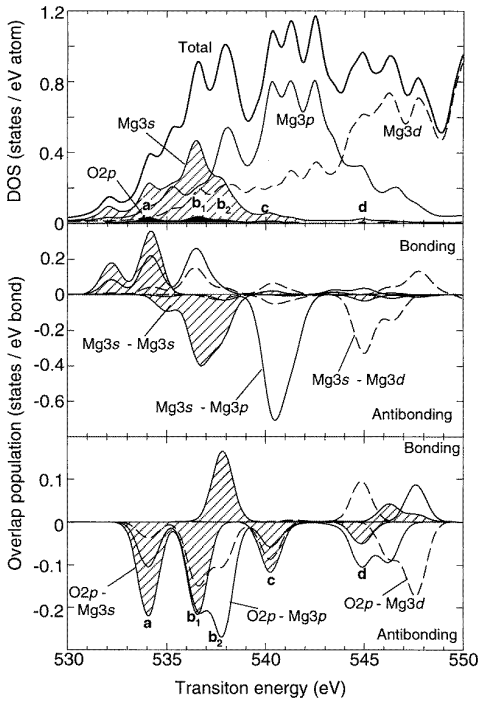

Figure 2. (Top) Density of states and bond overlap population diagrams of (middle) Mg 3s–Mg 3spd, and (bottom) O 2p–Mg 3spd calculated for the Slater transition state of the $(O_{13}Mg_{14})^{2+}$ cluster.

4. Effects of Si solutes in MgO

In order to examine the effect of Si^{4+} dissolution into MgO on the O K-edge PACS, Mg^{2+} is substituted by Si^{4+} without introducing any charge-compensating defects for simplicity to begin with. Lattice relaxation around Si^{4+} is not included, either. Figure 4 shows O 2p PDOS in comparison with cation PDOSs for two kinds of cluster at the Slater transition state. A Mg atom located at one of the nearest neighbour sites of the central oxygen atom is substituted by an Si atom. Extra features in the O 2p PDOS that is originated from Si–O interactions are denoted by a′ and b′. Similar to the case of Mg–O interaction, they can be ascribed to the Si 3s–O 2p antibonding and Si 3p–O 2p antibonding interactions, respectively. Peak a′ appears approximately 7 eV lower in the transition energy than the peak a.

The separation between peak a and a′ is found to be strongly dependent on the Si–O bond length. The ionic radius of Si^{4+} is 54 pm when coordinated by six ligands, whereas it is 86 pm for Mg^{2+} [14]. The Si–O bond length in the unrelaxed model is therefore 32 pm longer than expected from the ionic radius. Figure 5 shows the dependence of the energies of peak a and a′ on the Si–O bond-length computed for a series of small model clusters, $(SiO_6Mg_{12}O_8)^0$. It should be noted that this cluster is different from that used in figure 4 in order to include the lattice relaxation in a simple manner. In this case, a model cluster was centred by an Si atom in order to include the relaxation in the simplest manner, as can be seen in the cluster model shown in figure 5. Atomic positions other than those of six oxygen atoms coordinating central Si atoms are fixed throughout the series of calculations.

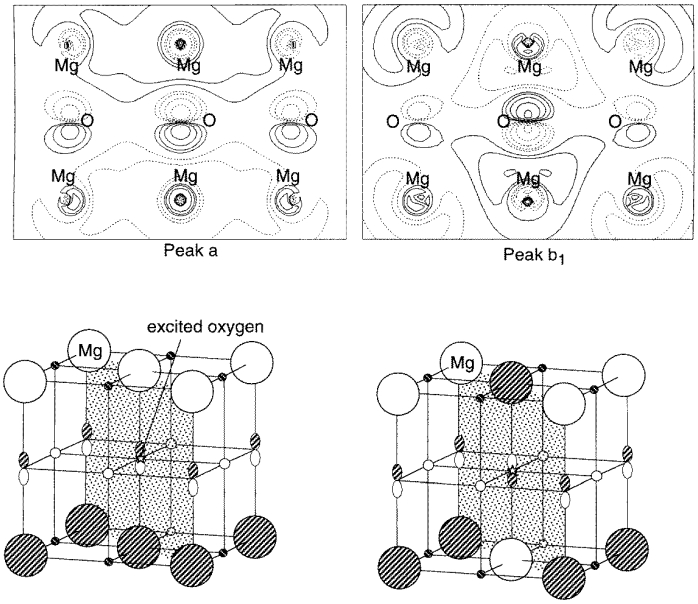

Figure 3. Contour maps of the wavefunctions on the (110) plane at peak a and b_1 in the $(O_{13}Mg_{14})^{2+}$ cluster for the Slater transition state. Curves are drawn for ± 0.015, ± 0.03, ± 0.06, ± 0.12 and ± 0.24, respectively. Solid and dotted curves are for positive values and negative values, respectively. Their schematic views are shown together. The dotted area corresponds to the contour map.

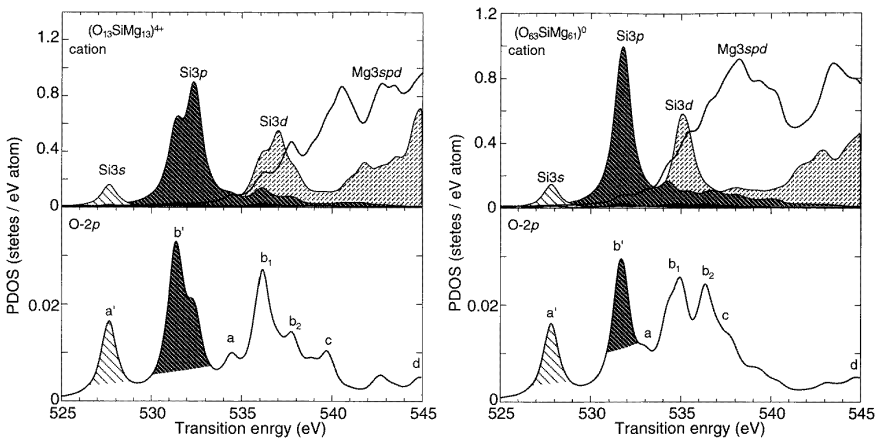

Figure 4. Unoccupied partial density of states for cation orbitals (top) and that for O 2p (bottom) calculated for Slater's transition state using two clusters that include Si (unrelaxed).

As can be seen in figure 5, the peak a′ exhibits strong dependence on the Si–O bond-length, whereas the peak a does not. The decrease of the Si–O bond-length has a dual effect on the increase of electrostatic potential at the oxygen site. One is simply the r^{-1} effect, the other is due to the increase of the net charge of Si, as can be seen in figure 5. Since the Si–O

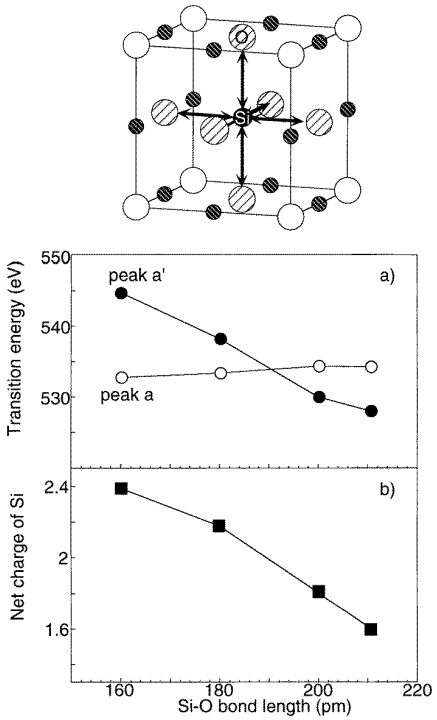

Figure 5. (a) Transition energy of the peak a and a′, and (b) net charge of Si as a function of Si–O bond length, calculated for the Slater transition state by the $(SiMg_{12}O_{14})^0$ cluster shown at the top.

bond-length in the unrelaxed model is much longer than the optimum, charge transfer from Si to O cannot be completed, thereby showing smaller ionicity.

When an Si^{4+} ion substitutes the Mg^{2+} site, an Mg^{2+} vacancy is likely to be introduced in order to maintain the charge neutrality. In order to include the effect of the Mg^{2+} vacancy, and also to include the atomic relaxation other than the nearest-neighbour sites, a total energy minimization using interatomic potentials has been conducted. An Mg^{2+} vacancy is put at one of the nearest cation sites of Si. The equilibrium lattice constant for pure MgO obtained by the present set of interatomic potentials is 410 pm, which is 97.4% of the experimental value.

A part of the optimized structure around Si is shown in figure 6. The Si–O bond-lengths are 175.9, 183.4 and 196.1 pm according to the optimization. The Si ion is slightly moved toward the Mg vacancy. The average Si–O bond length is 185.1 pm, which is 4.1% greater than the average Si–O bond length in stishovite, 177.5 pm. Stishovite is the only SiO_2 crystal having sixfold coordinated Si.

Since the equilibrium lattice constant of MgO is 2.6% smaller than that determined by experiment, the effect of the artificial compression should be known before the analysis of the optimized structure. The O K-edge PDOSs for undoped and Si-doped MgO (unrelaxed, no vacancy) using small clusters composed of 27 atoms having two different lattice constants are compared in figure 7. Although the compression brings about the shift in the transition energy by approximately 1 eV toward higher transition energy, the spectral shape does not change remarkably. This is also the case for the Si-doped cluster. We can therefore use the compressed MgO cluster as a reference to compare with the optimized structure shown in figure 6.

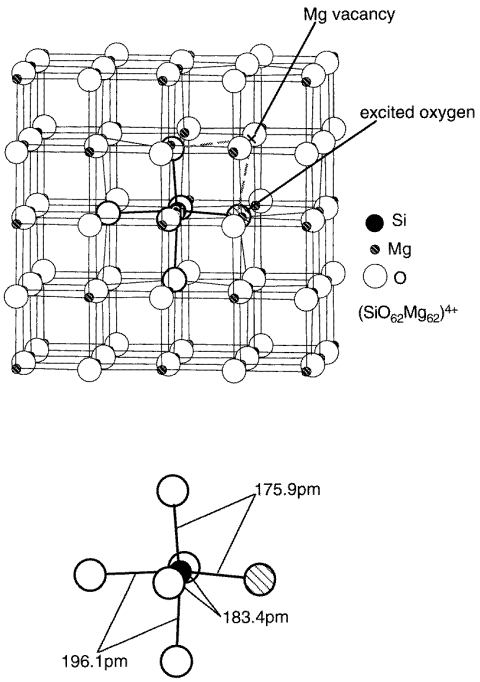

Figure 6. Atomic arrangement around an Si solute and an Mg vacancy optimized by energy minimization.

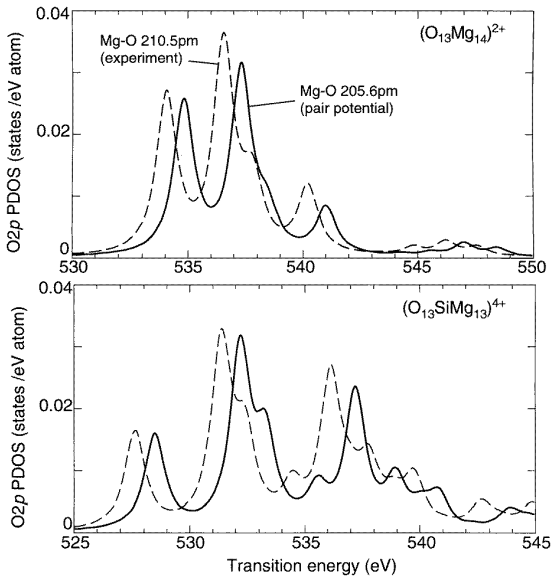

Figure 7. Effect of lattice constant on the O 2p PDOS by model clusters composed of 27 atoms. Top: $(O_{13}Mg_{14})^{2+}$ cluster. Bottom: $(O_{13}SiMg_{13})^{4+}$ cluster. Solid and broken curves correspond to Mg–O distances of 205.6 and 210.5 pm, respectively.

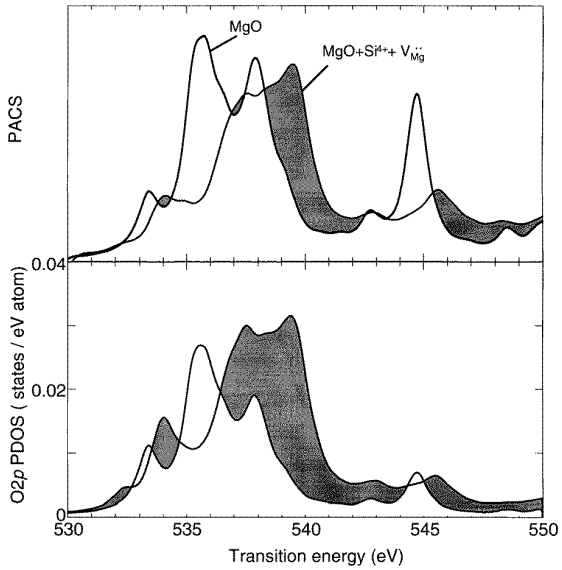

Figure 8. Comparisons of O K-edge PACS and O 2p PDOS between undoped and Si^{+4} + V''_{Mg}-doped MgO calculated by model clusters composed of 125 and 124 atoms for the Slater transition rate.

Figure 8 compares the O K-edge PACS and O 2p PDOS of undoped MgO (using Mg–O distance of 205.6 pm) and the optimized structure shown in figure 6. Calculations were made for model clusters with 125 and 124 atoms at the Slater transition state. A half-filled core hole is introduced into an oxygen atom located at the common neighbour of the Si and Mg vacancy (see figure 6). The hatched area shown in the theoretical PACS is expected to be seen by experiment if the geometry is correct. Because of the reduction of the Si–O bond length, peak a′ is expected to be much closer to peak a as compared with the unrelaxed model. In addition, peak a′ becomes broader because of the presence of three Si–O bond lengths. Shapes and energies of peak a and b also change because of the presence of the Mg vacancy. The extra feature in the theoretical O K-edge PACS due to the presence of the Si^{4+} and Mg vacancy is then expected to be located mainly at the higher-energy shoulder of the main peaks.

5. Summary

First-principles molecular orbital calculations using model clusters are made in order to understand the way to change the O K-edge ELNES by the presence of Si^{4+} solutes in the MgO host. Major results can be summarized as follows:

(1) Experimental O K-edge ELNES of undoped MgO is satisfactorily reproduced by calculation of PACS for a cluster composed of 27 atoms when a half-filled core hole is included. The reproduction is improved when the cluster size is expanded to 125 atoms. All spectral features up to 20 eV from the edge, denoted by peaks a to d, are interpreted from the viewpoint of Mg–O and Mg–Mg interactions.

(2) Extra features denoted by a′ and b′ appear by the substitution of Mg^{2+} by Si^{4+}. Positions of these peaks are found to be strongly dependent on the Si–O bond length. Therefore, the extra-peak position can be used as a good measure for the local environment of Si.

(3) Relaxation around the Si solute in MgO is evaluated by total energy minimization using interatomic potentials. When an Mg vacancy is introduced in order to maintain the charge neutrality the Si ion is expected to move toward the Mg vacancy. The average Si–O bond length is 185.1 pm. Theoretical O K-edge PACS of the relaxed structure found that the extra feature appears mainly at the higher-energy shoulder of the main peak. This may only be detected by careful experiments.

Acknowledgments

J D Gale for allowing us to use the GULP program and S Nagano for technical assistance are gratefully acknowledged. This work was supported by a Grant-in-Aid for General Scientific Research from the Ministry of Education, Sports, Science and Culture of Japan.

References

[1] Schlaudt C M and Roy D M 1965 *J. Am. Ceram. Soc.* **48** 248
[2] Kaneko K, Tanaka I and Yoshiya M 1998 *Appl. Phys. Lett.* **72** 191
[3] Tanaka I, Kawai J and Adachi H 1995 *Solid State Commun.* **93** 533
[4] Tanaka I, Nakajima T, Kawai J, Adachi H, Gu H and Rühle M 1997 *Phil. Mag. Lett.* **75** 21
[5] Tanaka I and Adachi H 1996 *Phys. Rev.* B **54** 4604
[6] Tanaka I and Adachi H1996 *J. Phys. D: Appl. Phys.* **29** 1725
[7] Kanda H, Yoshiya M, Oba F, Ogasawara K, Adachi H and Tanaka I 1998 *Phys. Rev.* B **58** 9693
[8] Adachi H, Tsukada M and Satoko C 1978 *J. Phys. Soc. Japan* **45** 875
[9] Ellis D E, Adachi H and Averill F W 1976 *Surf. Sci.* **58** 497
[10] Slater J C 1974 *Quantum Theory of Molecules and Solids* vol 4 (New York: McGraw-Hill)
[11] Gale J D 1997 *JCS Faraday Trans.* **93** 629
[12] Kawamura K 1992 *Molecular Dynamics Simulations (Springer Series in Solid State Sciences 103)* ed F Yonezawa (Berlin: Springer) pp 88–97
[13] Lindner T, Sauer H, Engel W and Kambe K 1986 *Phys. Rev.* B **33** 22
[14] Shannon R D 1976 *Acta Crystallogr.* A **32** 751